Hindawi
International Journal of Analytical Chemistry
Volume 2022, Article ID 5169548, 7 pages
https://doi.org/10.1155/2022/5169548

Research Article

Load Test Analysis of a Long-Span Prestressed Nano-Concrete Highway Bridge

Liang Yan

Shandong Hi-speed Transportion Construction Group Co.,Ltd., Jinan 250014, Shandong, China

Correspondence should be addressed to Liang Yan; z17301049@stu.ahu.edu.cn

Received 19 August 2022; Revised 7 September 2022; Accepted 19 September 2022; Published 30 September 2022

Academic Editor: Nagamalai Vasimalai

In order to solve the problem of vehicle-bridge coupling vibration of a continuous semisteel bridge, the main bridge type of long-span prestressed concrete girder bridge, the author proposes a bridge safety test system based on the dynamic and static load test. The system combines the change of stress and deflection with the vibration amplitude of the bridge body, and using the modeling assistant in large-scale finite element software MIDAS/CIVIL, a three-dimensional finite element real bridge model is established, including input of section data, the input of boundary conditions, and the input of loads. The result obtained is as follows: the structural verification coefficient of the control strain of the main girder under each working condition is not greater than 1.0, indicating that the flexural rigidity of the structure meets the design requirements. In addition, under each working condition, the ratio of the residual strain after unloading to the measured total strain is less than 20%. Under each working condition, the deflection calibration coefficient of each control section is less than 1.0, and the ratio of residual deflection to total deflection of each measuring point is at most 3.9%; each residual deflection is small. The damping ratios are all less than 5% of the empirical damping ratio of concrete members, indicating that the bridge structure is in good condition. The result obtained by the author is compared with the standard allowable value and the theoretical calculation value, so as to provide a basis for the study of the bearing capacity of similar bridges and to verify the standardization and rationality of the existing bridge structural design.

1. Introduction

With the advancement of science and technology and the improvement of the national economic level, China's bridge construction has entered a glorious period [1]. As early as 2005, the total mileage of highways in China reached 1.9 million km, the total mileage of expressways exceeded 35,000 km, and the total number of highway bridges exceeded 330,000 [2]. Many long-span bridges also came into being but with the increase in span, from several hundred meters to 3000 meters; the height-span ratio of the stiffening beam is getting smaller and smaller (1/40~1/300); the safety factor also decreases, from previous 4~5 to 2~3. The defects in the design and construction of existing bridges in China and the damage, aging, or disasters in the long-term use process are gradually exposed, and many problems such as cracking of concrete structures, reduced service performance, insufficient bearing capacity, and poor seismic performance have seriously affected the service life and structural safety of existing road network structures [3], and with the emergence of overweight equipment transportation, due to the limitation of the design load level of some bridges, especially those built in the early days, the load level cannot meet the needs of overweight equipment transportation. Due to the lack of necessary monitoring and corresponding maintenance, a large number of bridge damage accidents have occurred around the world, causing huge losses to the national economy, life, and property [4].

On August 13, 1997, the Tixi Tuojiang Bridge in Fenghuang County, western Hunan Province, collapsed on the eve of its completion after two years of construction. 63 people escaped, and 22 of them were injured. It has been confirmed that 47 people died unintentionally, and more than a dozen people are still crushed under the gravel, with no hope of survival. In October 1994, a major accident occurred in Seoul, South Korea, in which the central section of the Seongsu Bridge spanning the Han River was broken by 50 m, of which 15 m fell into the river, causing 32 deaths and

17 serious injuries. It is said that the reason for the sudden rupture of the bridge during rush hour is the long-term overload operation and fatigue failure of steel beam bolts and rods. The Tacoma Narrows Bridge, with a main span of 853 m, completed in 1940, was only used for three months, and the bridge collapse accident was caused by a wind speed of 19 m/s. In 1951, the Golden Gate Bridge with a main span of 1280 m was partially damaged due to vibration when the wind speed was 15~1520 m/s. Of approximately 500,000 highway bridges in the United States, more than 200,000 have varying degrees of damage. In February 1967, the Silver Bridge over the Ohio River suddenly collapsed, killing 46 people.

In order to ensure the quality of these bridges that cost a lot and are closely related to the national economy and people's livelihood, especially the quality of some new structural bridges and bridges using new materials and new construction techniques, according to the requirements of the "Technical Specifications for Highway Maintenance" promulgated by the Ministry of Communications, these bridges must be evaluated for their capacity [5, 6]. However, due to the difference between theoretical inference and actual structure characteristics, the identification of bearing capacity is still inseparable from the load test. The bridge load test is the most direct and effective method and means to evaluate the quality of bridges.

2. Literature Review

The development of prestressed concrete bridges was still in its infancy before the Second World War, but it is transitioning to the mature stage [7]. After World War II, many Western European countries such as the Federal Republic of Germany and France were damaged by the war, and a large number of bridges were in urgent need of repair. At that time, there was a shortage of steel after the war, which objectively provided very favorable conditions for the development of prestressed concrete bridges [8]. In order to avoid importing expensive steel materials from abroad, some third world countries in Africa and Latin America also give priority to prestressed concrete bridge schemes [9].

Once the prestressed concrete bridge jumped onto the historical stage of bridge construction, it showed its strong competitiveness. A record spanning over 100 m has been created since the 1950s. In the early 1960s, the erection method and the pushing method were applied to the middle span prestressed concrete continuous beam. For the long span prestressed concrete continuous beam, the application of various more perfect cantilever construction methods makes the continuous beam abandoned the expensive full floor construction method. Instead, an economical and effective highly mechanized construction method is adopted, so that the continuous beam scheme obtains new competitiveness and gradually occupies a dominant position in the range of 40m~200m [10, 11]. The 1953 Kochertal Bridge in the Federal Republic of Germany is an elevated multi-span continuous beam with a pier height of 183 m, a span arrangement of $81 + 7 * 138 + 81$ m, and a bridge deck width of 31 m. Only a single box with a width of 8.6 m is used, a long cantilever is lifted out of the box, and there is a diagonal brace to support the cantilever bridge deck every 7.66 m. Whether it is an urban bridge, an elevated road, a valley viaduct, or a bridge spanning a wide river, the prestressed concrete continuous beam has exerted its advantages, which often replaces other systems and becomes the winning solution of choice. From the 1970s to the 1980s, statistics were made on more than 200 prestressed concrete beam bridges with a main span greater than 100 m, and continuous beams accounted for 50% of the total [12].

The structural systems of prestressed concrete bridges in China already include simply supported beams, T-shaped rigid frames with hinges or hanging beams, continuous beams, truss arches, truss beams, and cable-stayed bridge systems. In highway and railway bridge projects, most of the simply supported beams above 20 m are made of prestressed concrete, and among the prestressed concrete bridges above medium span, cable-stayed bridges, T-shaped rigid-frame bridges, continuous girder bridges, truss arches, and truss girder (T-frame) bridges have been built [13]. The construction methods used are cantilever pouring and cantilever assembly method, jacking method, mobile formwork method, and large floating crane, erection, and rotation construction method [14].

The development of prestressed concrete truss bridges in China is also catching up with the world's advanced level [15]. The prestressed concrete cantilever truss bridge with the largest span is the Huanglingji Bridge (upper bearing type) in Hanyang, Hubei Province, built in 1979, with a main span of 90 m, and the cantilever truss arch bridge is the Jianhe Bridge in Guizhou Province, which was built in 1985, with a main span of 150 m. Currently, the under-supported cantilever truss girder bridge has the characteristics of rigid stay cables (the upper chord of the cantilever truss), as well as the characteristics of the truss, and the building height is small, which is more suitable for urban bridge engineering. The completed test bridge is the Zhejiang Port Bridge with a main span of 70 m. The main span of the Fujian Gongtang Bridge is 120 m [16, 17]. At present, research on the long-span prestressed concrete cable-stayed bridge is underway, and it is expected to approach or catch up with the world's advanced level; however, we must make arduous efforts in the design theory, construction technology and construction machinery, high-strength materials, and large-scale anchoring and tensioning systems of long-span prestressed concrete bridges [18].

The construction of prestressed concrete continuous bridges in China has been widely developed in the past 20 years, the spanning capacity of bridges has been continuously improved, and the structural system of continuous girder bridges has increased. Building materials, anchors, supports, and expansion joints used have all new developments. Construction technology and equipment are continuously improved and updated [19]. For this reason, continuous girder bridges have become one of the main types of prestressed concrete bridges. Continuous girder bridges are mainly divided into the following structural systems: continuous girder bridge, continuous rigid frame bridge, rigid frame-continuous composite girder bridge, etc.

Constant-section continuous girder bridges are mostly used for medium-span bridges and can be constructed by prefabricated installation, jacking method, and hole-by-hole construction. Variable-section continuous girder bridges are mostly used for long-span prestressed concrete continuous girder bridges [20].

The research on disease diagnosis and prevention of concrete bridge structures is one of the main directions of bridge research. The analysis of the bridge disease, the research, experiment and practice of the bridge detection, and identification method and the treatment of the bridge disease have attracted worldwide attention, and the international specialized institutions have been set up to study, and an international specialized institution has been established to conduct research.

For testing of bridges, many countries in the world are currently conducting research and experiments. In the mid-to-late 1980s, the United States installed corresponding detection devices on many of its large bridges to collect physical parameters such as displacement, strain, and acceleration of structures and components, as well as the impact of environmental factors on the structure. In the 1990s, the Lantan Fined Crossing Bridge and the Tsing Ma Bridge in Hong Kong, the Humen Bridge in Guangzhou, the Xupu Bridge in Shanghai, the Jiangyin Yangtze River Bridge, and the Nanjing Second Yangtze River Bridge were all installed with monitoring equipment during construction, which enabled real-time monitoring of structures during operation. Among them, the monitoring system of the Humen Bridge is composed of strain gauges, acceleration sensors, temperature sensors, displacement sensors (capacitive acceleration sensors), and GPS systems, on the basis of the construction monitoring and the bridge test system, the short-term operation monitoring of the bridge after a period of opening to traffic can be carried out, and these works will play a crucial role in ensuring the safe operation of bridges, extending their service life, and early detection of bridge diseases, in order to save the maintenance cost of the bridge and improve the comprehensive utilization efficiency of the bridge.

To sum up, in view of the influence of local stress such as diaphragms and chamfers at the pier-beam junction of high-pier and large-span continuous rigid-frame bridges, the stress is relatively complex, and the local stress analysis is carried out on the section near the midspan fulcrum and the pier bottom section so as to determine the sensitive element of the complex section. Then, through the load test, the research on the bearing capacity evaluation technology of the high pier and long-span prestressed concrete continuous rigid frame bridge is studied, and the calculation result of the sensitive element stress is verified and has important practical significance.

3. Research Methods

3.1. Equivalent Test Load. The design load of high-pier and long-span continuous rigid-frame bridges is often a vehicle with a superclass of 20, and a load of an automobile with a superclass of 20 is composed of a fleet of heavy trucks with axle loads of 30 tons and 55 tons arranged at certain intervals. During the field load test, due to various conditions, it is often difficult to accurately use standard loads to simulate loading of real bridges, the loading vehicles used are usually determined according to site conditions, and their actual axle loads and gross weights are usually different from standard loads.

The calculation of the test load effect is a process of determining the loading position, the loading level, and the size of the structure under the action of the test load on the basis of the calculation results of the design internal force or stress, and it is also a process of repeated trial calculation. In principle, since the bridge static load test is an identification load test, the test load should be the same as the design standard load as much as possible; however, due to the limitation of objective conditions, the actual test load is often difficult to be consistent with the design standard load. Under the premise of not affecting the main test purpose, the loading method equivalent to internal force, stress, or deformation is generally used; that is, the most unfavorable internal force or stress generated by the design standard load on the control section is calculated, and it is used as the control value; then, the test load is adjusted so that the internal force or stress of the section can reach this control value step by step. In order to ensure the test effect, according to the requirements of the "Test Method for Large-Span Concrete Bridges," when selecting the test load size and loading position, the static load test efficiency η should be used for regulation, that is,

$$\eta = \frac{S_t}{(S_d(1+\mu))}. \tag{1}$$

In the formula, S_t is the calculated value of the deformation or internal force and stress of the detection part under the action of the test load.

S_d under the action of the design standard load is the calculated value of the deformation or internal force and stress of the detection part.

μ is the impact coefficient taken by the design.

The value of η should be between 0.8 and 1.05. When the bridge investigation and verification work are relatively complete, the lower limit value of η can be adopted. When the bridge investigation and verification work are insufficient, especially when the design and calculation data are lacking, the high limit value of η can be adopted. The η constant table of the bridge static load test efficiency is shown in Table 1.

3.2. Static Load Test. The test preparation stage is the premise and guarantee for the bridge load test to be carried out smoothly. The work at this stage includes the collection of bridge technical data such as bridge design documents, construction records, supervision records, original test data, and bridge maintenance and repair records; the current status of the bridge, such as the apparent inspection of the deck system, load-bearing structural members, supports, and foundations; and theoretical checking and calculation of the internal force under the action of the design load and the

Table 1: Efficiency constant table of the bridge static load test.

Type of bridge	Stress calibration factor	Deflection check factor
Reinforced concrete slab bridge	0.2–0.4	0.2–0.5
Reinforced concrete girder bridge	0.4–0.8	0.5–0.9
Prestressed concrete bridge	0.6–0.9	0.7–1.0

test proposed load, such as the formulation of the loading plan, the formulation of the measurement plan, and the selection of instruments and meters. It also includes on-site preparations such as erecting working scaffolds, setting up measuring instrument brackets, measuring point stacking and surface treatment, testing component layout, and installation and debugging of measuring instruments.

The loading and observation stage is the central part of the whole testing work. The work at this stage is based on the preparations in place, and according to the predetermined test plan and test procedure, suitable loading equipment to load is used, various test instruments are used, various performance indicators of the test structure after being stressed are observed, such as deflection, strain, crack width, and acceleration, and manual recording or automatic instrument recording means to record various observation data and information are used. The specific layout is shown in Figure 1.

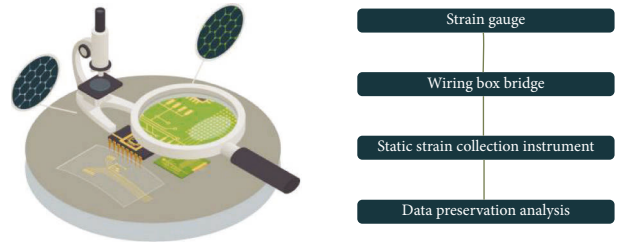

Figure 1: Schematic diagram of the site layout of static load test data collection.

3.3. Dynamic Load Test. Some parameters of bridge structure dynamic performance, such as natural frequency, damping ratio, mode shape, dynamic impact coefficient, and dynamic response, are important indicators for macroscopically evaluating the overall stiffness and operational performance of bridge structures. It is also the main criterion for some norms to evaluate the safety operation performance of bridges. At present, although there is no unified evaluation scale for the dynamic response and dynamic characteristics of bridge structures in domestic and foreign codes, it is generally believed that the dynamic characteristics of a bridge structure reflect the overall stiffness of the structure, the flatness of the bridge deck, and the ability to dissipate external vibration energy input. At the same time, excessive dynamic response will affect safe driving of the vehicle and cause discomfort to the driver and passengers, which should be avoided. The field layout of the dynamic load test is shown in Figure 2.

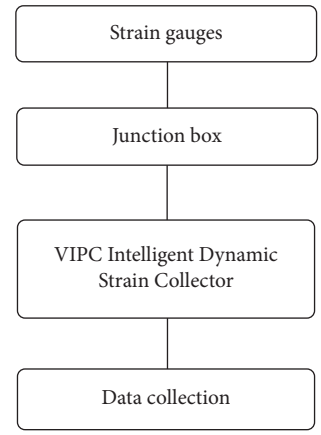

Figure 2: Schematic diagram of the site layout for the data collection of the dynamic load test.

The following factors can evaluate the dynamic performance of bridge structures:

(1) The theoretically calculated and measured values of the frequency of the bridge structure are compared, and if the measured value is greater than the theoretically calculated value, it means that the actual stiffness of the bridge structure is relatively large; otherwise, it means that the stiffness of the bridge structure is relatively small, and there may be cracks or other abnormal phenomena. In general, some assumptions are often made when theoretical calculations are performed and some secondary factors are ignored; therefore, the theoretically calculated value is greater than the measured value.

(2) The driving performance of the bridge structure is evaluated according to the measured value of the dynamic impact coefficient. If the measured impact coefficient is large, it means that the driving performance of the bridge structure is poor, and the flatness of the bridge deck is poor, and vice versa.

(3) To evaluate the driving comfort of the bridge structure according to the magnitude of the measured acceleration and research data at home and abroad, generally, the maximum vertical acceleration of the vehicle when driving on the bridge structure should not exceed g (g is the acceleration of gravity); otherwise, it will cause discomfort to drivers and passengers.

(4) The magnitude of the measured damping ratio reflects the ability of the bridge structure to dissipate external energy input, and if the damping ratio is large, it means that the bridge structure has strong ability to dissipate external energy input, and the vibration attenuates quickly. If the damping ratio is small, it means that the bridge structure has poor

ability to dissipate external energy input, and vibration decays slowly. However, if the damping ratio is too large, the bridge structure may be cracked or the working condition of bearing is abnormal.

3.4. Finite Element Modeling. The continuous rigid frame system is a complex spatial force system, and obviously, it is very difficult to analyze and solve it by the analytical method. In recent years, with the increasing application of electronic computers in engineering, favorable conditions have been provided for numerical methods to solve complex spatial structures. The finite element method is a numerical solution method that developed rapidly with the advent of computers and has been widely used in engineering analysis in recent years.

For bridge structures, the most important thing is the longitudinal force analysis of the structure. Considering that the span-to-width ratio of bridges is generally relatively large, it is a practical method to approximate the longitudinal analysis model as a member system. The commonly used bridge software is based on the general program of the finite element of the plane rod system, and special software is developed according to the characteristics of the structure, construction, and design of bridge engineering.

ANSYS has the function of cell life and death. This option is used in bridge structural analysis to simulate the bridge construction process. The function of unit generation is equivalent to erecting bridge components, and the function of unit death is equivalent to demolishing bridge components. In addition, ANSYS also has the function of programming, through which the design and analysis of various bridge schemes can be simulated into a simple and labor-saving process. Compared with the traditional modeling methods, the use of program modeling can obtain fast, accurate, and convenient calculation methods and calculation results.

4. Analysis of Results

4.1. Static Load Test. The main span structure of the bridge in the author's test is a large-span prestressed concrete semi-rigid frame and a continuous box girder. When selecting test items, the characteristics of continuous girder bridges should be fully considered. The main items tested are the side span of the continuous box girder bridge, the maximum positive bending moment in the middle span, the positive bending distance at the 1/4 section of the middle span, and the maximum negative bending moment at the fulcrum.

There are 5 test conditions on the left and right sides of the bridge static load test, and the detailed introduction of each condition is as follows:

(1) Working condition 1 : 8 loading vehicles are arranged in 4 rows and 2 columns, the transverse bridge is symmetrically loaded, and the longitudinal arrangement is at the most unfavorable loading position of the positive bending moment in the middle of the side span.

(2) Working condition 2 : 8 loading vehicles are arranged in 4 rows and 2 columns, the load is symmetrically distributed across the bridge, and the longitudinal arrangement is at the most unfavorable loading position of the negative bending moment of the top section of the pier on the west side.

(3) Working condition 3 : 8 loading vehicles are arranged in 4 rows and 2 columns, the transverse bridge is symmetrically loaded, and the longitudinal arrangement is at the most unfavorable loading position of the positive bending moment of the midspan 1/4 section.

(4) Working condition 4 : 8 loading vehicles are arranged in 4 rows and 2 columns, the transverse bridge is symmetrically loaded, and the longitudinal arrangement is at the most unfavorable loading position of the midspan positive bending moment.

(5) Working condition 5 : 8 loading vehicles are arranged in 4 rows and 2 columns, the transverse bridge is eccentrically loaded, and the longitudinal arrangement is at the most unfavorable loading position of the negative bending moment in the middle span.

The static load conditions and efficiency coefficients of the bridge after calculation are shown in Table 2.

The static load test was carried out to obtain the data, and the residual strain test results under each working condition were calculated as shown in Table 3.

As can be seen from Table 3, the structural verification coefficient of the control strain of the main girder under each working condition is not greater than 1.0, indicating that the flexural rigidity of the structure meets the design requirements. In addition, under each working condition, the ratio of the residual strain after unloading to the measured total strain is less than 20%, which meets the requirements of the "Test Method for Large-Span Concrete Bridges." It shows that the stress state of the structure is in the linear elastic working range. The participating deflections under each working condition in the static load test are shown in Figure 3.

Figure 3 shows that under each working condition, the deflection calibration coefficient of each control section is less than 1.0, the maximum ratio of residual deflection to total deflection of each measuring point is 3.9%, and each residual deflection is small, indicating that the vertical stiffness of the bridge satisfies design requirements.

4.2. Dynamic Load Test

4.2.1. Sports Car Test. A 30 t car was used to pass through the bridge-span structure at a constant speed back and forth at speeds of 20 km/h, 30 km/h, 40 km/h, and 50 km/h, respectively, in order to determine the forced vibration response of bridge structures under dynamic loads. The results of the sports car experiment are shown in Figure 4.

Spectrum calculation and analysis on sports car test data were performed, and it can be seen that the frequency components of each measuring point in the sports car test are mainly concentrated around 3.15 Hz.

Table 2: Static load conditions and efficiency coefficients.

Working conditions	Number of test cars	Control item	Load factor	Efficiency factor
1	8	Positive bending moment	0.972	Symmetry
2	8	Negative bending moment	0.943	Symmetry
3	8	Positive bending moment	0.883	Symmetry
4	8	Positive bending moment	0.892	Symmetry
5	8	Positive bending moment	0.894	Partial load

Table 3: Residual strain of the control section.

Working conditions	1	2	3	4	5
Residual strain	3	1	0	2	1
Total strain	61	68	43	66	69
Residual/real	4.91%	1.47%	0	3.03%	1.45%

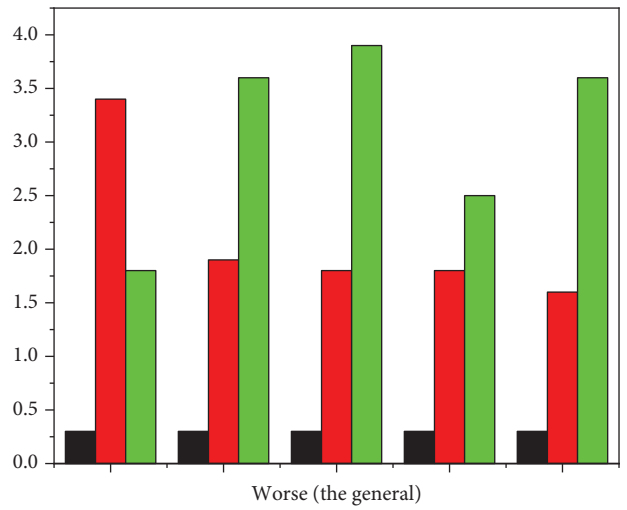

Figure 3: Total deflection under each working condition.

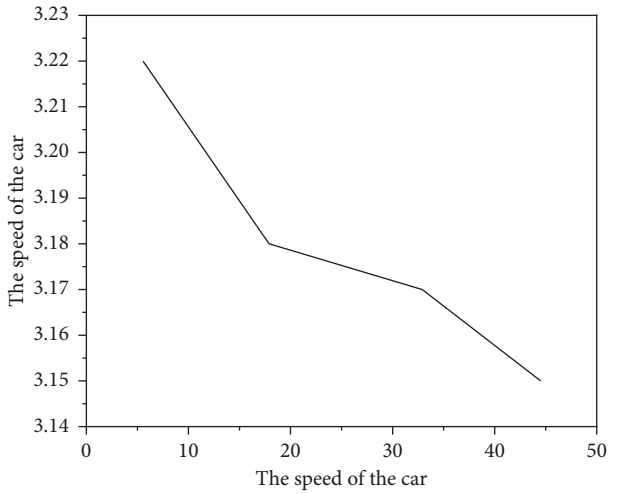

Figure 4: The main frequencies of the sports car test at no speed.

4.2.2. Jump Test. By establishing a finite element model, the damping ratio of the bridge during the dynamic load test is analyzed, and during the test, in the bridge-span structure, a 10 cm-high triangular dunnage is set on the bridge deck in the middle of the span, so that the 30T car can cross the obstacles at 3 km/h, 5 km/h, and 7 km/h, determining the forced vibration response of bridge structures under dynamic loads. The results of the jump test are shown in Figure 5.

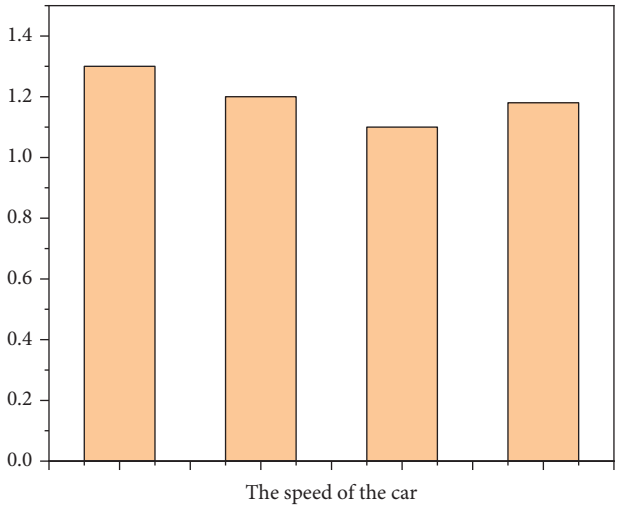

Figure 5: Bridge damping ratio at different vehicle speeds.

From the analysis of the above test data, it can be seen that the damping ratio decreases with the increase of vehicle speed, and the calculated damping ratio is less than 5% of the empirical damping ratio of concrete members, indicating that the bridge structure is in good condition.

5. Conclusion

The author systematically introduces the main contents of static and dynamic load tests, summarizes the relevant theories, introduces the field test and the processing analysis of the test data in detail, and introduces the relevant theories for the evaluation of the test results. The mechanical performance of the bridge structure was compared and systematically tested, and the test data that could reflect the overall mechanical performance of the structure were obtained; the dynamic load test frequency with two test items of the sports car and jumping car was compared and analyzed, and the damping ratio in the jumping car was analyzed.

The conclusion is drawn as follows:

(1) In the static load test, the residual stress of the test bridge span after unloading is less than that specified in the "Test Method for Large-Span Concrete Bridges." It shows that the superstructure of the test span is in an elastic working state.

(2) In the dynamic load test, under the condition of symmetrical load and eccentric load, the deflection value of the bridge deck on both sides of the test bridge has a good linear relationship and eccentric load correlation with the loading level, and the maximum deflection of the midspan section under the test load is much smaller than the calculated value (1/600) according to stiffness theory, indicating that the stiffness of the test bridge span meets the requirements. The residual deflection value of each measuring point after unloading is very small, and no cracks were seen during the experiment, indicating that the bridge superstructure was within the elastic working range.

Data Availability

The data used to support the findings of this study are available from the corresponding author upon request.

Conflicts of Interest

The author declares that there are no conflicts of interest.

References

[1] C. Song, G. Zhang, W. Hou, and S. He, "Performance of prestressed concrete box bridge girders under hydrocarbon fire exposure," *Advances in Structural Engineering*, vol. 23, no. 8, pp. 1521–1533, 2020.

[2] C. J. Naito, "Construction and field evaluation of electrically isolated tendons in a prestressed concrete spliced girder bridge," *Journal of Bridge Engineering*, vol. 25, no. 7, pp. 1–9, 2020.

[3] D. Tonelli, M. Luchetta, F. Rossi, P. Migliorino, and D. Zonta, "Structural health monitoring based on acoustic emissions: validation on a prestressed concrete bridge tested to failure," *Sensors*, vol. 20, no. 24, p. 7272, 2020.

[4] S. Yifan, H. Wenliang, Y. Yangguang, and R. Shipu, "Strengthening prestressed concrete box girder bridge by upgrading structural system," *Journal of Performance of Constructed Facilities*, vol. 34, no. 1, Article ID 04019103, 2020.

[5] R. Anay, A. Lane, D. V. Jáuregui, B. D. Weldon, V. Soltangharaei, and P. Ziehl, "On-site acoustic-emission monitoring for a prestressed concrete bt-54 aashto girder bridge," *Journal of Performance of Constructed Facilities*, vol. 34, no. 3, Article ID 04020034, 2020.

[6] H. Jiang, X. Dong, Z. Fang, J. Xiao, and Y. Chen, "Experimental study on shear behavior of a uhpc connection between adjacent precast prestressed concrete voided beams," *Journal of Bridge Engineering*, vol. 25, no. 12, Article ID 04020106, 2020.

[7] C. Sim, M. Tadros, D. Gee, and M. Asaad, "Flexural design of precast, prestressed ultra-high-performance concrete members," *PCI Journal*, vol. 65, no. 6, pp. 35–61, 2020.

[8] N. P. Thulaseedharan and M. T. Yarnold, "Prioritization of Texas prestressed concrete bridges for future truck platoon loading," *Bridge Structures*, vol. 16, no. 4, pp. 155–167, 2021.

[9] S. S. Srinivasan, M. Rung, and R. D. Ferron, "Factors affecting loss in durability in prestressed-concrete girders with microcracking," *Journal of Bridge Engineering*, vol. 25, no. 9, Article ID 04020068, 2020.

[10] T. S. Eom, E. J. Park, and S. J. Lee, "Shear behavior of reinforced concrete structural walls under eccentric compression load," *ACI Structural Journal*, vol. 117, no. 1, pp. 63–73, 2019.

[11] R. W. Alemayehu, Y. Kim, J. Bae, and Y. K. Ju, "Cyclic load test and finite element analysis of novel buckling-restrained brace," *Materials*, vol. 13, no. 22, p. 5103, 2020.

[12] C. G. Kim, T. S. Eom, and H. G. Park, "Cyclic load test of reinforced concrete columns with v-shaped ties," *ACI Structural Journal*, vol. 117, no. 3, pp. 91–102, 2020.

[13] S. Yang, J. Zhou, Z. Bian, and Z. Xu, "Point-load test method for estimation of in situ masonry mortar strength," *Journal of Materials in Civil Engineering*, vol. 32, no. 10, Article ID 04020286, 2020.

[14] H. J. Kim, H. J. Hwang, and H. G. Park, "Eccentric-axial-load test for composite columns using bolt-connected steel angles," *Journal of Structural Engineering*, vol. 146, no. 9, Article ID 04020178, 2020.

[15] A. Kurnyta, W. Zielinski, P. Reymer, K. Dragan, and M. Dziendzikowski, "Numerical and experimental uav structure investigation by pre-flight load test," *Sensors*, vol. 20, no. 11, p. 3014, 2020.

[16] M. Fan and A. Sharma, "Design and implementation of construction cost prediction model based on svm and lssvm in industries 4.0," *International Journal of Intelligent Computing and Cybernetics*, vol. 14, no. 2, pp. 145–157, 2021.

[17] M. S. Pradeep Raj, P. Manimegalai, P. Ajay, and J. Amose, "Lipid data acquisition for devices treatment of coronary diseases health stuff on the internet of medical things," *Journal of Physics: Conference Series*, vol. 1937, no. 1, Article ID 012038, 2021.

[18] X. L. Zhao, X. Liu, J. Liu, J. Chen, S. Fu, and F. Zhong, "The effect of ionization energy and hydrogen weight fraction on the non-thermal plasma vocs removal efficiency," *Journal of Physics D Applied Physics*, vol. 52, no. 14, 2019.

[19] R. Huang and X. Yang, "Analysis and research hotspots of ceramic materials in textile application," *Journal of Ceramic Processing Research*, vol. 23, no. 3, pp. 312–319, 2022.

[20] Q. Zhang, "Relay vibration protection simulation experimental platform based on signal reconstruction of MATLAB software," *Nonlinear Engineering*, vol. 10, no. 1, pp. 461–468, 2021.